# ADAPTIVE NON-RIGID REGISTRATION OF 3D KNEE MRI IN DIFFERENT POSE SPACES

*Taehyun Rhee*[1]*, *J.P. Lewis*[3], *Krishna Nayak*[2], *Ulrich Neumann*[1]

[1]Department of Computer Science, University of Southern California, Los Angeles, USA
[2]Department of Electrical Engineering, University of Southern California, Los Angeles, USA
[3]Weta Digital, Wellington, New Zealand

## ABSTRACT

Volume registration of articulated subjects such as the human knee region requires novel methods to accommodate the wide range of movement resulting from skeletal joint rotations. This paper addresses articulated volume deformation with a pair of techniques. Volume skeletal deformation (VSD) is applied first, producing a smooth but approximate deformation of the soft tissue as the underlying skeleton moves, while preserving rigid motion in the segmented bone regions. The resulting deformed volume is used as initialization for a non-rigid deformation step that locally and adaptively adds radial basis function control points to minimize the remaining registration error in any poorly aligned region. The resulting process registers a neutral pose volume to any given bent-knee pose MRI scan.

***Index Terms***— adaptive registration, non-rigid registration, articulation, volume deformation, MRI

## 1. INTRODUCTION

Articulated bodies such as the human knee have a wide range of skeletal movements, resulting in large motion and deformations of the surrounding soft tissue. Quantifications and measurements of such deformation is important for bio-medical applications and clinical studies such as motion analysis of patients suffering from arthritis.

The goal of quantifying the movement in a set of volume scans can be approached with non-rigid volume registration. Registration methods based only on the raw intensity data have obvious benefits, since these methods operate directly on the image intensity values without using any fiducial markers or prior data reduction and segmentation by user [1, 2].

Non-rigid volume registration requires high degree of freedom (DOF) warping functions for smooth, continuous, and shear-free deformation of the soft-tissue volumes [3]. Rueckert et al. registered 3D breast MRIs while optimizing normalized mutual information (MI) [4]. The initial locations were positioned by rigid global affine transformations, and the volumes were smoothly warped to the targets using optimization of B-splines based free-form deformation (FFD).

*Thanks to Samsung Electronics for support.

Although the B-splines create locally supported smooth deformations, using a regular grid of control points results in many DOF in optimization. Recently, adaptive registration has been studied to reduce DOFs and computation times. Rohde et al. used the gradient of global mutual information (MI) to find mismatching regions. Wu's radial basis functions (RBF) successfully supported smooth volume deformation using irregularly allocated sparse control points [5]. Locally measured normalized MI was used by Park et al. to identify highly mismatched regions requiring additional control points [6]. The radial basis function formulation of thin plate splines (TPS) was used for deformation. In this paper, their efforts are successfully extended to handle articulated deformation, using the VSD algorithm [7] as an initialization step.

Previous non-rigid registration studies have been generally focused on non-articulated subjects such as the brain [5, 6] and breast [4]. Articulated subjects involve a much wider range of deformation, and are best approached with methods that explicitly model the effect of movement of the underlying bones. However, rigid transformation alone is not sufficient to produce the desired smooth deformation, nor even to provide an adequate initialization for non-rigid deformation algorithms (Fig. 1).

Martin-Fernandez et al. presented elastic registration of human hand X-rays using a 2D articulated registration approach. A simple wire model is manually created based on the inner skeleton structure and the images are deformed based on the weights calculated by a distance measure from the wire [8]. Papademetris et al. presented a rigid body registration method for serial lower-limb mouse CT images. They addressed the importance of the initialization step in intensity based non-rigid body registration and present a method to initialize a model to any arbitrary posture [9]. Li et al. presented articulated whole body registration of serial micro CT mouse images. Pose initialization is accomplished using point-based registration algorithms operating on the bone point clouds.

Skin surface deformation arising from articulated body animation has been a major topic in surface-based computer graphics. One widely used class of methods is that inspired by the Skeletal Subspace Deformation or linear blend skinning algorithm [10, 11]. Rhee et al. developed volume skeletal deformation (VSD) which provides a practical solution to ar-

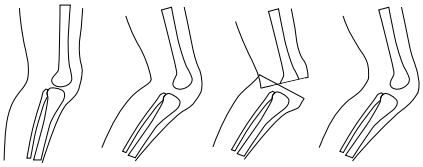

**Fig. 1**. From left, (a) schematic source (neutral pose) scan, (b) target pose, (c) rigid transformation does not provide adequate initialization for non-rigid registration, (d) VSD produces an approximate but suitable initialization (c.f. Fig. 3 (c)).

ticulated volume animation. VSD produces rigid bone movement and smooth volumetric tissue deformation as the actual segmented skeleton moves under intuitive user control [7].

Efficient intensity-based registration of volume scans from articulated subjects is a challenging task, both because of the many DOF involved and because the large range of movement means registration targets are well outside the capture range of optimization approaches using downhill search. For example, knee MRI volumes in different poses show large differences between the source (straight-knee) volume $V_s$ and the target (bent-knee) volume $V_t$.

In this paper, we provide a practical solution to solve this problem and show sufficient registration results using in vivo 3D MRI. The VSD algorithm is modified to produce an initial volume at a given target pose which may have large pose differences from the source volume. Then, the initialized source volume is continuously warped to the target volume using adaptive non-rigid volume registration based on intensity similarity optimization. Since it uses adaptively allocated sparse control points in mismatched regions, the overall DOF of volume registration is efficiently constrained.

## 2. ARTICULATED VOLUME INITIALIZATION

The volume skeletal deformation (VSD) algorithm [7] is implemented for articulated volume pose initialization. The VSD algorithm is based on the linear weighted blending of affine transforms determined by each joint,

$$v_a = (\sum_{j=1}^{m} w_j M_j) v_s \tag{1}$$

where $m$ is the number of joints, $v_s$ is a voxel in a source pose, $v_a$ is a deformed voxel in an arbitrary pose $a$, $M_j$ is a homogeneous $4\times4$ transformation matrix that transfers joint $j$ from the source pose to an arbitrary pose in world coordinates, and $w_j$ is a joint weight that defines the contribution of joint $j$'s transformations to the deformation. The volumetric weight map to define $w_j$ is computed using a generic surface model and bone joint weights [7], and the transformation matrix $M_j$ that represents the target pose is estimated from the bone locations of the target volume. In the source knee volume, the femur and tibia are manually segmented by a 2D graph cut algorithm [12]. The segmented bones are then registered to the target volume using intensity based rigid volume registration minimizing the squared sum of intensity differences (SSID),

$$\min_{M_j} |I_s(M_j V_j) - I_t(V_t)|^2 \tag{2}$$

where $I_s$ is the intensity of bone volume $V_j$ transferred by matrix $M_j$, and $I_t$ is the intensity of target volume. Although MI would be better for multi-modal images, since we have a single modality, SSID is adequate for our initialization.

## 3. ADAPTIVE NON-RIGID REGISTRATION

After articulated initialization, the task turns out to be a problem of non-rigid volume registration. We define a cost function to minimize mismatch between volumes as,

$$\min_{\mathbf{f}} S(V_s^l,\ V_t^l + T(V_t^l, \mathbf{c}, \mathbf{f})),\ \text{for all levels } l \tag{3}$$

where $S$ is a similarity measure such as SSID or MI (in case of MI the value should be maximized), $V_s^l$ is a source volume at level $l$, $V_t^l$ is a target volume at level $l$, $T$ is a warping function to determine the needed additional deformation of volume $V_t$, $\mathbf{c}$ is a control point vector assigned at the target volume frame, $\mathbf{f}$ is the displacement value of the related control point ($\mathbf{c}$, $\mathbf{f}$ are discussed further below) and $l$ is the level of a multi-resolution volume that is constructed from the original volume to speed up processing and avoid local minimum.

For registration of a large volume, the DOF of vector $\mathbf{c}$ and $\mathbf{f}$ should be constrained. In order to decrease DOF, control points are adaptively allocated in regions of large mismatch. Therefore, the deformation function $T$ should allow sparse irregular control points and their displacement values. Given a set of irregular feature locations (control points) $\mathbf{c}$ = $\{c_1, ..., c_n\}$ and their values $\mathbf{f}$ = $\{f_1(c_1), ..., f_n(c_n)\}$ we can find a function $R(x)$ which gives smooth interpolation of these feature values using radial basis functions (RBFs) [13].

$$R(x) = P(x) + \sum_{i=1}^{n} \lambda_i \phi(|x - c_i|) \tag{4}$$

We choose the RBFs to determine the deformation function $T$, where $P(x)$ is a low-degree polynomial, $\lambda_i$ is a real valued weight, $\phi$ is a basis function, $x$ is an arbitrary 3D location, $|x - c_i|$ is the Euclidian distance between $x$ and $c_i$, and $f_i$ is the displacement value at $c_i$. For the basis function, the 3D thin plate spline (TPS) $\phi(r) = |r|$ is chosen for smooth and continuous deformation, since the TPS interpolates specified values while minimizing an approximate curvature [14].

The control points of the RBFs are adaptively assigned, increasing DOF only in areas of local dissimilarity [6]. Each target volume $V_t^l$ is hierarchically divided into multiple cells with the hierarchy level denoted $b$; the coarsest level $b_{min}$ contains 2x2x2 cells. The maximum number of cells at the finest level $b_{max}$ is constrained by the resolution of the $V_t^l$ to

control the total number of control points; e.g. volumes having larger than 64x64x64 resolution can have 16x16x16 cells at level $b_{max}$. If the size of a cell is too small, the histogram-based local MI measure by Park et al. [6] may not be accurate. In this case, SSID is used since all our scans have the same modality.

In every cell at level $b$ ($b \in b_{min} \ldots b_{max}$), whenever the similarity measure of each cell is less than a given threshold, a control point $c_i$ ($i^{th}$ point) is added at the center of the cell in the target volume space and the value $f_i$ is initialized by the RBF deformation $T$ defined by the previous **c** and **f**. After increasing the DOF of **c** and **f**, the cost function in equation (3) is optimized with respect to **f**, producing the desired displacement value for each control point. If the cost is not decreased enough during optimization or the SSID of all cells are larger than a given threshold, the cell level $b$ is increased (up to $b_{max}$). Because TPS interpolation is global, it is also necessary to ensure that the added local deformations do not influence regions that are already well aligned. Thus, at cell level $b_{min}$, a control point is assigned at the center of each cell (eight total) and a similar number of control points are allocated at iso-surfaces of each bone volume which have been segmented and initialized in section 2.

## 4. RESULTS

Sufficiently different poses of knee MRI volumes were captured from a male volunteer. A GE Signa Excite 3.0 T scanner with gradients capable of 40 mT/m amplitude and 150 T/m/s slew rate was used. The data set for each volume is approximately 136x256x256 and the spatial resolution of each voxel is 1.25x1.25x1.2 ($mm^3$). Two different tests were performed to show the robustness of our methods.

First, we registered synthetically posed volumes with small pose variations and no articulated VSD initialization, in order to verify the adaptive non-rigid registration in a setting where the ground truth is known. Voxels identified to be inside the base volume $V_s$ are stored in a separate one-dimensional list termed the *representative volume*. The representative volume is bent 10 degrees using the VSD algorithm to create a target arbitrary pose. The deformed irregular voxels are then re-sampled from $V_s$ to construct target volume $V_t$. Since the geometric topology between representative volumes is the same, the registration error can be measured using the Euclidean norm between the two representative volumes.

The result of adaptive non-rigid registration is shown in figure 2. The total number of allocated control points is small (less than 30) and they are shown in the Fig. 2 (c); blue dots show control points in the target space, red dots show correspondences in the source space, and lines show the displacements. Since hierarchical multi-resolution volumes are used, the largest differences are minimized while registering the coarse resolution volume. Therefore, the displacement values are decreasing with increasing resolution; Fig. 2 (c) is the result for a 34x64x64 resolution volume. The mean Euclidean distance between the source and target volume is reduced from 10.5 to 3.2 ($mm^3$). The correlation of the two image volumes is improved from 0.54 to 0.95. 99.8% of registered representative voxels are located within a four voxel distance of the (known) target voxel and 87% are within two voxels; refer the voxel spatial resolution. Although the knee volume was just bent 10 degrees, the difference between the volumes is relatively large compared with non-articulated subjects such as the brain and breast. The registration algorithm shows accurate results with small numbers of control points considering that intensity values were approximated using trilinear interpolation.

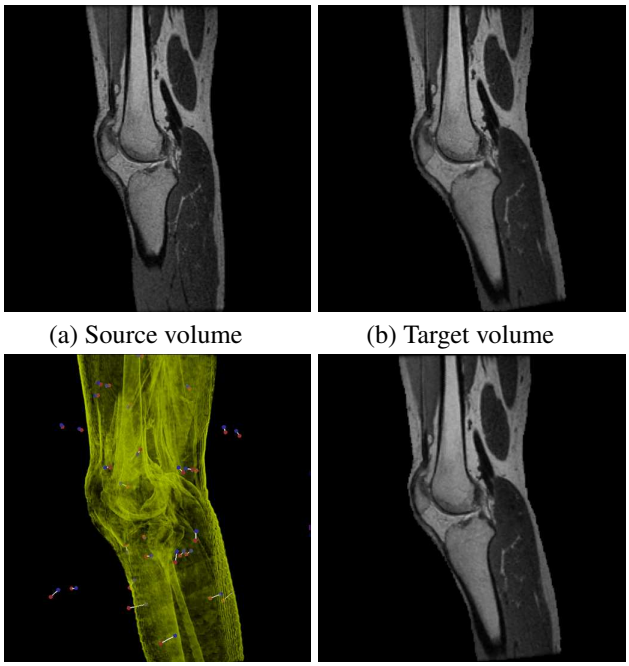

(a) Source volume (b) Target volume

(c) Control points (d) Registration

**Fig. 2**. 3D registration of synthetic ground truth data without VSD pose initialization.

Next, we registered real 3D knee MRIs with significantly different poses. A source volume is manipulated to the target pose using the VSD articulated volume initialization (Fig. 3 (c)). The initialized volume then registered to the target volume using the adaptive non-rigid registration method. The registration result is shown in Fig. 3 (d) and visually validated in Fig. 3 (f); red dots show the registered source voxel grids on a slice of the target volume shown in gray. Around 22 control points are adaptively assigned. The control points, corresponding points, and their displacement values are shown in Fig. 3 (e); the sub-volume resolution is 68x128x128.

## 5. CONCLUSION

A practical solution to register MRI scans from an articulated, moving subject is presented and demonstrated on the human

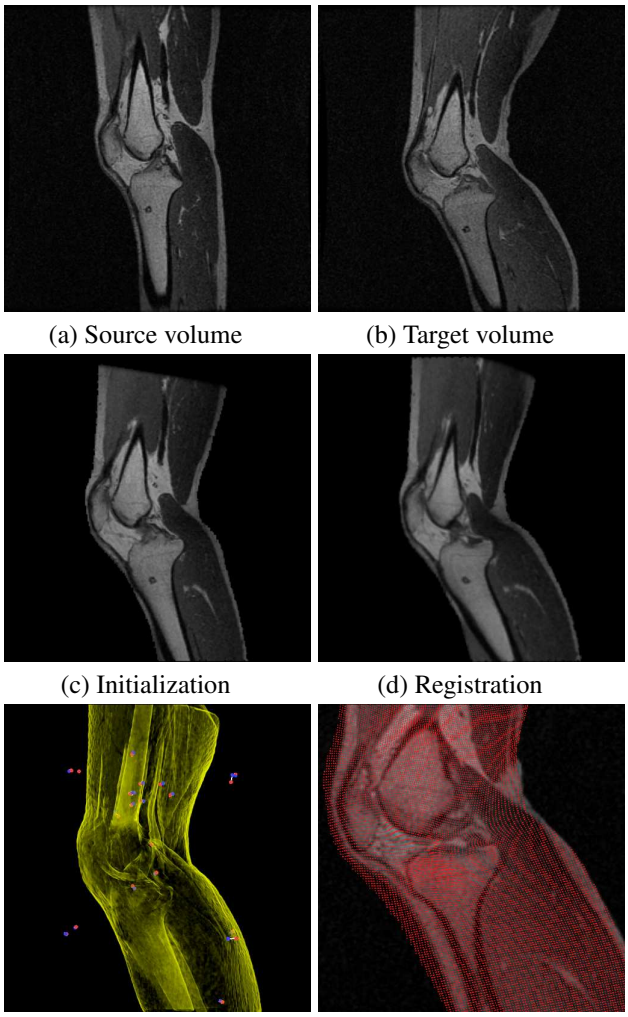

(a) Source volume (b) Target volume

(c) Initialization (d) Registration

(e) Control points (f) Comparison

**Fig. 3**. 3D registration of real 3D MRI knee scans.

knee region. Articulated volume initialization based on the VSD algorithm produces good initial poses for non-rigid registration. The initialized volume is then aligned to the target volume using non-rigid volume registration with adaptively allocated sparse control points. The results are tested on in vivo 3D knee MRIs and show robust results even among volumes with significantly different poses.

Based on the articulated characteristics of the in vivo subject, we encountered some problems which have not been common issues in the previous registration studies. Since the subject's pose is changing, the body region covered by each scan can be different, and regions existing only in a single scan cannot contribute to the registration and cause slow optimization. In order to reduce discomfort during scans, the patient laid facing upward and supported by some casts. Therefore, the soft-tissue volume on the back side is compressed. Although our articulated volume initialization could approximate muscle bulging, soft tissues compressed by patient weight could not be restored. If MRI volumes were captured in some specific poses considering these issues, better results can be achieved. However, the trade off between ideal data and patient comfort may be a good discussion issue in this study.

## 6. REFERENCES


[1] J. Maintz and M. Viergever, "A survey of medical image registration," *Medical Image Analysis*, vol. 2, no. 1, pp. 1–36, 1998.

[2] J. V. Hajnal, D. L.G. Hill, and D. J. Hawkes, *Medical Image Registration*, CRC Press, 2001.

[3] T. McInerney and D. Terzopoulos, "Deformable models in medical images analysis: a survey," *Medical Image Analysis 1(2)*, pp. 91–108, 1996.

[4] D. Rueckert, L. I. Sonoda, C. Hayes, D. L. Hill, M. O. Leach, and D. J. Hawkes, "Nonrigid registration using free-form deformations: application to breast MR images.," *IEEE Trans Med Imaging*, vol. 18, no. 8, pp. 712–721, August 1999.

[5] G. K. Rohde, A. Aldroubi, and B. M. Dawant, "The adaptive bases algorithm for intensity-based nonrigid image registration," *IEEE Trans. Medical Imaging*, vol. 22, pp. 1470–1479, 2003.

[6] H. Park, P. H. Bland, K. K. Brock, and C. R. Meyer, "Adaptive registration using local information measures," *Medical Image Analysis 8(4)*, pp. 465–473, 2004.

[7] T. Rhee, J.P. Lewis, U. Neumann, and K. Nayak, "Soft-tissue deformation for in-vivo volume animaton," in *Proc. of Pacific Graphics*, 2007, pp. 435–438.

[8] M. A. Martin-Fernandez, E. Munoz-Moreno, M. Martin-Fernandez, and C. Alberola-Lopez, "Articulated registration: Elastic registration based on a wire-model," in *Medical Imaging 2005: Image Processing*. February 12–17 2005, pp. 182–191, SPIE Press, Proc. of the SPIE 5747.

[9] X. Papademetris, D.P. Dione, L.W. Dobrucki, L.H. Staib, and A.J. Sinusas, "Articulated rigid registration for serial lower-limb mouse imaging," 2005, pp. 919–926, MICCAI'05.

[10] N. Magnenat-Thalmann, R. Laperrière, and D. Thalmann, "Joint–dependent local deformations for hand animation and object grasping," in *Graphics Interface*, 1988, pp. 26–33.

[11] A. Mohr, L. Tokheim, and M. Gleicher, "Direct manipulation of interactive character skins," in *SI3D '03: Proc. Symposium on Interactive 3D graphics*. 2003, pp. 27–30, ACM Press.

[12] C. Rother, V. Kolmogorov, and A. Blake, "GrabCut: interactive foreground extraction using iterated graph cuts," in *ACM SIGGRAPH*. 2004, pp. 309–314, ACM Press.

[13] J. Carr, R. Beatson, J. Cherrie, T. Mitchell, W. R. Fright, B. McCallum, and T. Evans, "Reconstruction and representation of 3D objects with radial basis functions," in *SIGGRAPH 2001, Computer Graphics Proceedings*. 2001, pp. 67–76, ACM Press / ACM SIGGRAPH.

[14] F. L. Bookstein, "Principal warps: Thin-plate splines and the decomposition of deformations," *IEEE. Trans. Pattern Analysis Machine Intelligence*, vol. 11, pp. 567–585, 1989.